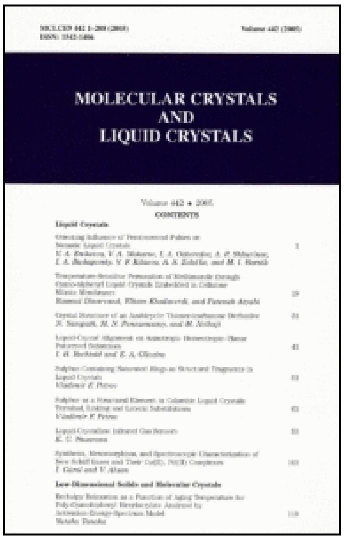

Molecular Crystals and Liquid Crystals
Publication details, including instructions for authors and subscription information:
http://www.informaworld.com/smpp/title~content=t713644168

Electrically Tunable Liquid Crystal Filters

Z. Raszewski[a]; E. Kruszelnicki-Nowinowski[a]; J. Kędzierski[a]; P. Perkowski[a]; W. Piecek[a]; R. Dąbrowski[b]; P. Morawiak[a]; K. Ogrodnik[a]
[a] Institute of Applied Physics, Military University of Technology, Warsaw, Poland [b] Institute of Chemistry, Military University of Technology, Warsaw, Poland

First published on: 13 July 2010

To cite this Article Raszewski, Z. , Kruszelnicki-Nowinowski, E. , Kędzierski, J. , Perkowski, P. , Piecek, W. , Dąbrowski, R. , Morawiak, P. and Ogrodnik, K.(2010) 'Electrically Tunable Liquid Crystal Filters', Molecular Crystals and Liquid Crystals, 525: 1, 112 — 127

To link to this Article: DOI: 10.1080/15421401003796132

URL: http://dx.doi.org/10.1080/15421401003796132

Mol. Cryst. Liq. Cryst., Vol. 525: pp. 112–127, 2010

ISSN: 1542-1406 print/1563-5287 online
DOI: 10.1080/15421401003796132

Electrically Tunable Liquid Crystal Filters

Z. RASZEWSKI,[1] E. KRUSZELNICKI-NOWINOWSKI,[1] J. KĘDZIERSKI,[1] P. PERKOWSKI,[1] W. PIECEK,[1] R. DĄBROWSKI,[2] P. MORAWIAK,[1] AND K. OGRODNIK[1]

[1]Institute of Applied Physics, Military University of Technology, Warsaw, Poland
[2]Institute of Chemistry, Military University of Technology, Warsaw, Poland

This paper presents tunable liquid crystal filter consists of three interference filters (LC – cells) with different cell thicknesses. These filters use nematic liquid crystal (with high birefringence). Such design allows to select precisely (using the electric field) the wavelength of outgoing light.

Keywords Interference filter; nematic liquid crystal; tunable filter

Introduction

NLC (Nematic Liquid Crystal) mixtures consisting isothiocyanato tolane and isothiocyanato terphenyl liquid crystals have been widely developed in our University. Some of them have got both: high optical ($\Delta n \leq 0{,}45$) and high dielectric ($\Delta\varepsilon \leq 20$) anisotropies and relatively low viscosity γ. Appling the mentioned above LC mixtures in HG (Homo Geneously aligned) cells with thickness d about 1 μm, 3 μm and 5 μm one can obtain the possibilities to develop FOETLCF (First Order Electrically Tunable Liquid Crystal Filter) and three stage ETLCF (Electrically Tunable Liquid Crystal Filter). These types of filters can gain some acceptance in astronomy and remote sensing pollution monitoring. A distinct advantage ETLCF over conventional tunable filters is possibility of construction ETLCFs with extremely large clear aperture, low power consumption and low addressing voltage.

- Due to the relatively high and electrically controlled (by applying U voltage) optical anisotropies $\Delta n(U)$ of used NLC and the cell gaps d (1 μm, 3 μm and 5 μm) the ETLCF can (easily) select the wanted wavelength $\lambda(U)$ not only from visible but near infrared range as well.

Address correspondence to Z. Raszewski, Institute of Applied Physics, Military University of Technology, Warsaw, Poland. Tel.: +48 22 685 74 27; E-mail: zraszewski@wat.edu.pl

- Due to high dielectric anisotropy $\Delta\varepsilon$, relatively low viscosity γ and small cell gap d, the ETLCF can achieve the response time shorter then 1 ms.

In this paper we describe and discuss our efforts in obtaining and optimization the ETLCFs.

I. Theory

In the laboratory system of coordinates Oxyz (see Fig. 1), a parallel to the Oz axis ray of unpolarized light of intensity I_0 strike normally the linear polarizer P followed by an ideally transparent birefringent object and the analyzer A. Let us consider a birefringent object in the form of homogeneously aligned nematic liquid crystal (NLC) layer of thickness d confined between two ITO electrodes (S_1 and S_2). This NLC layer is equivalent to a layer with optical axis laying parallel to the surfaces S_1 and S_2. The intensity transmittance of both polarizers is τ [1]. The planes of polarizer P, analyzer A and ITO electrodes are parallel to the Oxy plane. When the molecular director **n** of NLC is parallel to the Ox axis and NLC possesses positive values of optical Δn and dielectric $\Delta\varepsilon$ anisotropies, the effective optical indicatrix and the ellipsoid of static electric permittivity of NLC look like the ellipsoids of revolution with long axes paralleled to **n**.

Under the above considerations, it can be shown [2–4] that the intensity I of light transmitted by the analyzer, after passing the distance of d in the birefringent object with optical anisotropy $\Delta n = n_e - n_o$ is given by:

$$I = 2I_o\tau^2\left[\cos^2(\alpha-\beta) - \sin 2\alpha \sin 2\beta \sin^2\frac{\pi d \Delta n}{\lambda}\right] \qquad (1)$$

where λ is the light wavelength taken into consideration.

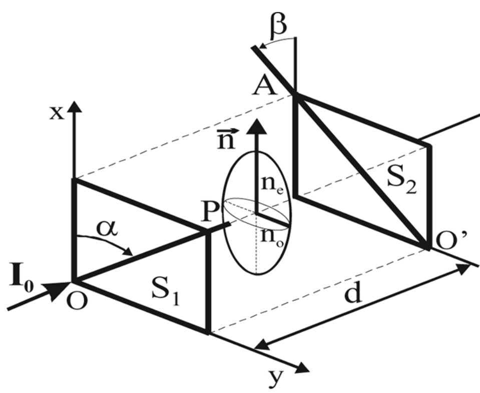

Figure 1. NLC layer of thickness d is confined between two S_1 and S_2 *ITO* electrodes. I_0 – the intensity of a ray of unpolarized light. The molecular director **n** of NLC is parallel to the Ox axis. OP and O'A are transmission axes of polarizer and analyzer. Directions OP and O'A of light vibration in the polarizer and analyzer form angels α and β with the Ox axis. n_e is the long and n_o is the short axis of optical indicatrix of NLC. n_e and n_o are extraordinary and ordinary refractive indexes of NLC respectively.

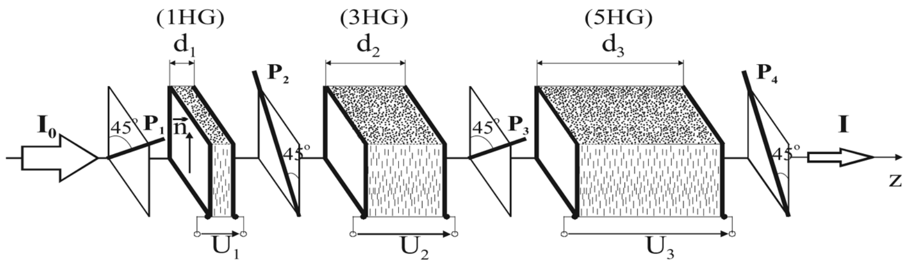

Figure 2. Schematic diagram of ETLCF, which contains 1HG, 3HG, and 5HG cells sandwiched between P_1, P_2, P_3, and P_4 polarizers. The birefringents of NLC layers in 1HG, 3HG and 5HG cells are guided by voltages U_1, U_2, and U_3 respectively.

For crossed polarizers (when $\alpha = 45°$ and $\beta = -45°$) and the diagonal position of birefringent NLC layer (when molecular director of NLC is parallel to the Ox axis) the Eq. (1) takes form:

$$\mathrm{I} = 2\mathrm{I_o}\tau^2 \sin^2\frac{\pi \mathrm{d}\Delta \mathrm{n}}{\lambda} = \mathrm{I_{max}} \sin^2\frac{\pi \mathrm{d}\Delta \mathrm{n}}{\lambda} \tag{2}$$

where $I_{\max} = 2\mathrm{I_o}\tau^2$ is the intensity of the light transmitted only by two polarizers.

If one computes, the effective transmission T given by (3)

$$\mathrm{T} = \frac{\mathrm{I}}{\mathrm{I_{max}}} = \sin^2\frac{\pi \mathrm{d}\Delta \mathrm{n}}{\lambda} \tag{3}$$

For $\mathrm{d}\Delta\mathrm{n} = 0.4\,\mu\mathrm{m}$ (which, for example, can by practically realized when one takes the NLC mixture with $\Delta\mathrm{n} = 0.4$ and then fill this NLC into 1HG (homogeneously

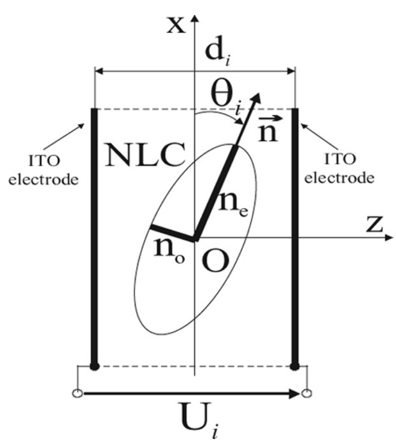

Figure 3. The voltage U_i is applied to the cell of thickness d_i (preliminary formed as HG) filled with NLC material. NLC is characterized by: K_{11} – splay elastic constant, γ – rotational viscosity, n_e – extraordinary and n_o – ordinary refractive indexes, perpendicular $\varepsilon_\perp$ – and parallel $\varepsilon_\parallel$ – components of permittivity tensor ε. In such boundaried NLC layer under voltage U_i, the vector field of directors $\mathbf{n}_i(z)$ is formed [5,6]. This director field, in the first approximations, can be characterized by average angle Θ_i.

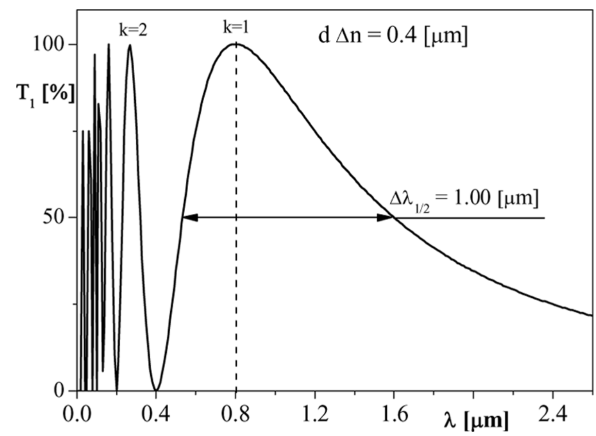

Figure 4. $T_1(\lambda)$ for $d\Delta n = 0.4\,\mu m$ in 1HG.

aligned) cell (with thickness d = 1 μm), one can obtain the results plotted in Figure 4. The spectrum $T_1(\lambda)$ shown in this figure for $d\Delta n = 0.4\,\mu m$ has got wide first order interference line at wavelength $\lambda = 0.8\,\mu m$. The half width $\Delta\lambda_{1/2}$ of this line (with interference index k = 1 for $(\frac{d\Delta n}{\lambda} = \frac{1}{2})$ is 1 μm.

If the factor of dΔn decreases (what can be practically realized by applying voltage U_1 to the 1HG cell with NLC), the maximum of the first order line shifts left in the wavelength domain. When the factor of dΔn equals 0.2 μm, the first order line is about two times thinner then it was in the case of $d\Delta n = 0.4\,\mu m$ and has its maximum at $\lambda = 0.4\,\mu m$, what is shown in Figure 5. In this place one can notice, that due to electrically controlled (by applying U_1 voltage) optical anisotropy $\Delta n(U_1)$, only the first order line appears in tunable range (from 0.4 μm to 0.8 μm). Such electrically tunable, 1 μm thick HG cell (with NLC characterized by relatively high optical anisotropy $\Delta n = 0.4$), can be regarded as First Order Electrically Tunable Liquid Crystal Filter (FOETLCF).

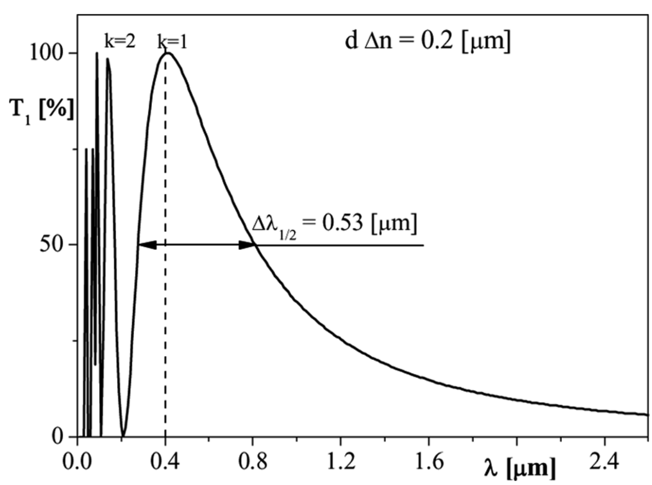

Figure 5. $T_1(\lambda)$ for $d\Delta n = 0.2\,\mu m$ in 1HG.

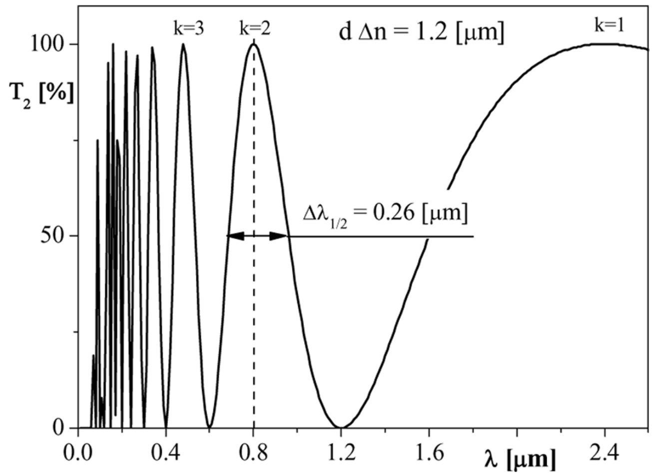

Figure 6. $T_2(\lambda)$ for $d\Delta n = 1.2\,\mu m$ in 3HG.

Figure 6 shows effective transmission $T_2(\lambda)$ obtained from (3), when $d\Delta n = 1.2\,\mu m$, what can be practically realized by $3\,\mu m$ thick cell (3HG) and NLC with $\Delta n = 0.4$. The second order interference line ($k = 2$ for $\frac{d\Delta n}{\lambda} = \frac{3}{2}$) has its maximum at $\lambda = 0.8\,\mu m$. When the factor of $d\Delta n$ decreases, what can be practically realized by applying voltage U_2 to the 3HG cell with NLC, the maximum of the second order line shifts towards the shorter wavelength. When the factor of $d\Delta n$ equals exactly $0.6\,\mu m$, the maximum of this line is at $\lambda = 0.4\,\mu m$, what is shown in Figure 7.

In Figure 8 transmission $T_3(\lambda)$ (calculated from (3)) is plotted for $d\Delta n = 2\,\mu m$, what can be practically achieved by $5\,\mu m$ thick cell (5HG) and NLC with $\Delta n = 0.4$. The third order interference line ($k = 3$ for $\frac{d\Delta n}{\lambda} = \frac{5}{2}$) reaches its maximum at $\lambda = 0.8\,\mu m$. If the value of $d\Delta n$ decreases (when voltage U_3 is applying to the 5HG cell with NLC), the maximum of the third order line shifts towards the shorter

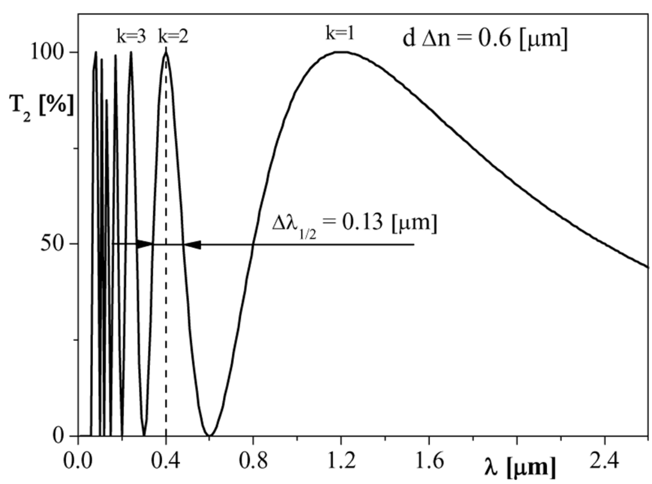

Figure 7. $T_2(\lambda)$ for $d\Delta n = 0.6\,\mu m$ in 3HG.

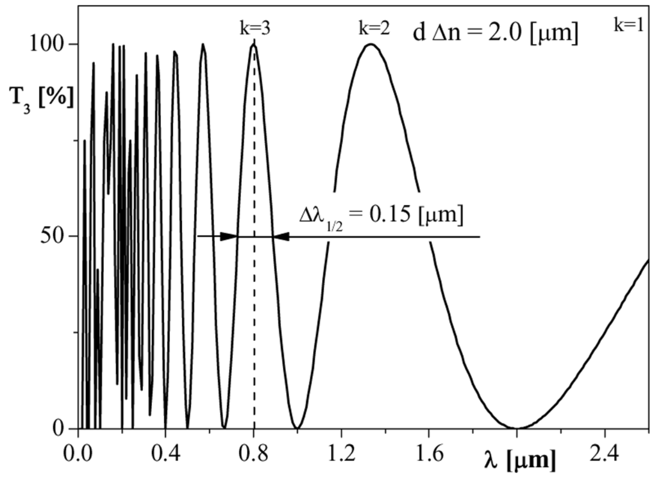

Figure 8. $T_3(\lambda)$ for $d\Delta n = 2\,\mu m$ in 5HG.

wavelength. When the factor of dΔn is 1 μm, the maximum of this line is placed at $\lambda = 0.4\,\mu m$, what is shown in Figure 9.

One can notice, that electrically forced (by U_2 voltage) shift of second order line (k = 2) in visible range from 0.4 μm to 0.8 μm is always accompanied by appearing two interference bands with k = 1 and k = 3 in visible range (see Figs. 6, 7). The same case is presented in Figures 8 and 9, where the shift (forced by U_3) of third order line (k = 3) in visible range is accompanied by three additional bands with k = 2, k = 4 and k = 5. On the other hand both transmission bands for k = 2 and k = 3 are much narrower then for k = 1.

Figure 2 shows the layout of Electrically Tunable Liquid Crystal Filter (ETLCF) which consists of three LC cells (1HG, 3HG, and 5HG) sandwiched between four polarizers. In such a filter, every cell is placed between crossed polarizers (every LC cell works in the birefringent system).

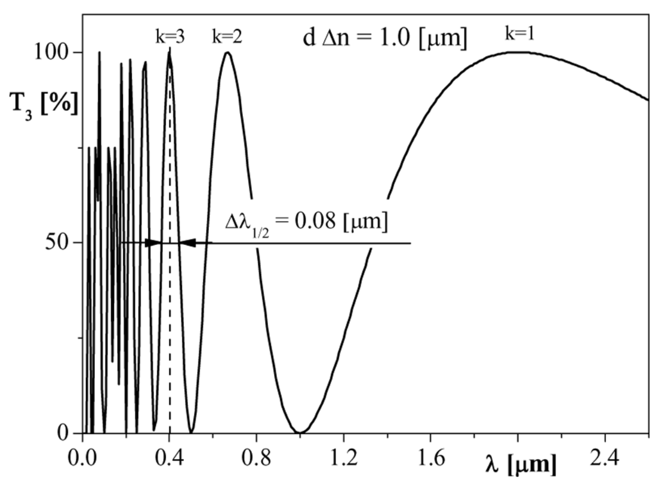

Figure 9. $T_3(\lambda)$ for $d\Delta n = 1\,\mu m$ in 5HG.

The intensity I of the light transmitted through such ETLCF is given by:

$$I = \left\{ \left[\left(2I_0\tau^2 \sin^2 \frac{\pi d_1 \Delta n_{1ef}}{\lambda} \right) 2\tau \sin^2 \frac{\pi d_2 \Delta n_{2ef}}{\lambda} \right] 2\tau \sin^2 \frac{\pi d_3 \Delta n_{3ef}}{\lambda} \right\} \tag{4}$$

where Δn_{ief} is the effective optical anisotropy, produced by applying U_i into HG cell with thickness d_i. In the first approximations Δn_{ief} can be given by [5]:

$$\Delta n_{ief} = \frac{n_o n_e}{\sqrt{n_o^2 \cos^2 \Theta_i + n_e^2 \sin^2 \Theta_i}} - n_o \tag{5}$$

where Θ_i is the average angle between optical director **n** and Ox axis established in the HG cell with thickness d_i under U_i voltage (see Fig. 3)

Using the Eq. (4), one can notice, that for $U_1 = U_2 = U_3 = 0$ applied to ETLCF where $d_1 = 1\ \mu m$, $d_2 = 3\ \mu m$, $d_3 = 5\ \mu m$ and all optical anisotropies of NLC layers are the same ($\Delta n_{1ef} = \Delta n_{2ef} = \Delta n_{3ef} = 0.4$), transmission T_{FO} of this filter can be written as:

$$T_{FO} = \frac{I}{I_{F\max}} \tag{6}$$

Knowing that: $T_1 = \sin^2 \frac{\pi d_1 \Delta n}{\lambda}$, $T_2 = \sin^2 \frac{\pi d_2 \Delta n}{\lambda}$, $T_3 = \sin^2 \frac{\pi d_3 \Delta n}{\lambda}$, Eq. (6) takes form:

$$T_{FO} = T_1 \cdot T_2 \cdot T_3 \tag{7}$$

where

$$I_{F\max} = 8I_0\tau^4 \tag{8}$$

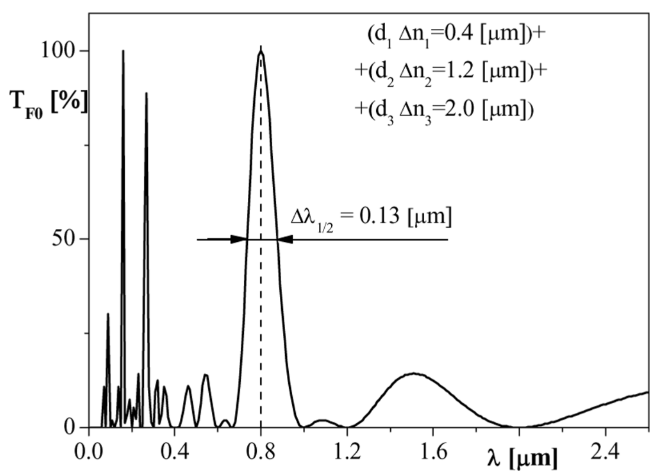

Figure 10. $T_{FO}(\lambda)$ for ETLCF without electric field ($U = 0$).

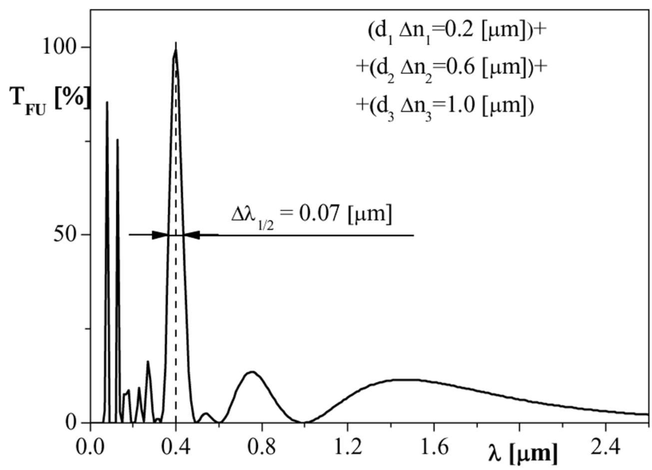

Figure 11. $T_{FU}(\lambda)$ for ETLCF under U_1, U_2, and U_3.

Figure 10 shows transmission spectrum T_{FO} calculated from (6) for three stage ETLCF when $d_1 = 1\,\mu m$, $d_1 = 3\,\mu m$, $d_1 = 5\,\mu m$ and $\Delta n_1 = \Delta n_2 = \Delta n_3 = 0.4$, while the Figure 11 presents transmission spectrum T_{FU} after applying guided voltages: U_1 to 1HG cell, U_2 to 3HG cell and U_3 to 5HG cells respectively. In ETLCF one can easily select (by applying electric voltages to the proper cells), the suitable wavelength $\lambda(U)$, from visible as well as near infrared range. In our three stage ETLCF the half width $\Delta\lambda_{1/2}$ of transmission band at $\lambda = 0.8\,\mu m$ is $0.13\,\mu m$, while at $\lambda = 0.4$ is much narrower ($0.07\,\mu m$).

If we suppose that our NLC is characterized by the following material parameters: $n_o = 1.5$, $n_e = 1.9$, $K_{11} = 10^{-12}\,N$, $\gamma = 150cP$, $\varepsilon_\perp = 4.0$ and $\varepsilon_\| = 19.0$ we can estimate the response time t_{ON} of our ETLCF. After putting the typical NLC to the 5HG cell (where $d = 5\,\mu m$) and applying $U = 5\,V$ we are able to switch the cell (to change the

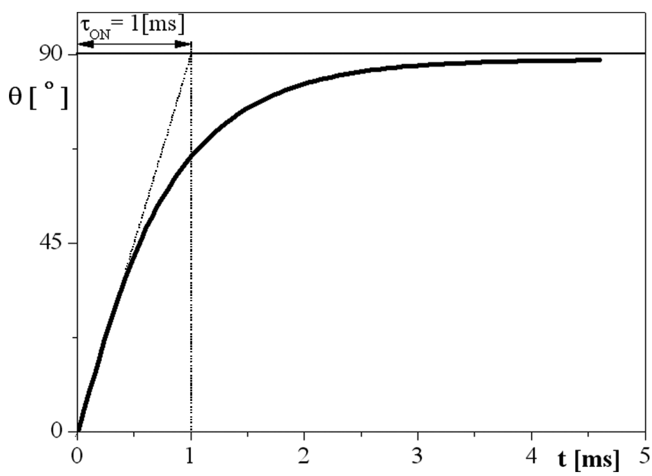

Figure 12. Switching process of NLC layer (with $\Delta\varepsilon = \varepsilon_\| - \varepsilon_\perp = 15.0$, $\gamma = 150cP$, $d = 5\,\mu m$) in 5HG cell under $U = 5\,V$.

angle Θ from 0° to 90°, see Fig. 3). Figure 12 shows the switching process in 5HG cell under U = 5 V. Value indicated in Figure 12: $\tau_{ON} = 1$ μs was estimated [7] from (9):

$$\tau_{ON} \propto \frac{\gamma d^2}{\Delta\varepsilon\varepsilon_o U^2} \tag{9}$$

From (5) one can learn out that to change Δn_{ef} from 0.4 to 0.2, Θ increases from 0° to 40°. So, the total response times t_{ON} for establishing given wavelength λ in our ETLCF, seems to be 1 μs or less.

Taking into account (8) and supposing that in our ETLCF all four polarizers are characterized by the same transmittance $\tau = 0.4$ [1], we can calculate the maximum of outgoing light intensity $I_{Fmax} = 8I_0\tau^4 = 0.2I_0$. One can find out that the intensity of the light transmitted through our (three stage) ETLCF states only 20% of incident light.

II. NLC Mixture for ETLCF

NLC mixtures consisting isothiocyanato tolane and isothiocyanato terphenyl liquid crystals have been widely developed in our University [12,13]. Using these experiences we tried to establish a new NLC mixture for ETLCF (farther called LCJ1791A) with $\Delta n \geq 0.4$, $\Delta\varepsilon \geq 15.0$ and the possible lowest viscosity γ in wide temperature range. The LCJ1791A mixture with phase sequence: Cr – 30.0°C – N –127.5°C – Iso was studied by electrooptic, dielectric, refractometric and microscopic means.

Dielectric properties of LCJ1791A were studied in isotropic and nematic phases over the frequency range from 100 Hz to 10 MHz, using IMPEDANCE ANALYZER HP 4192A. To do it the special measuring cells with golden electrodes were applied. The thickness of measuring cells was d = 8 μm, while the active area of electrodes was S = 1 cm^2 [8]. Temperature dependences of $\varepsilon_{||}(T)$, $\varepsilon_{\perp}(T)$ and $\varepsilon_I(T)$ are shown in Figure 13.

The refractive indices; isotropic – n_I, ordinary – n_o and extraordinary – n_e were measured using combined methods. applying both appropriately prepared Abbe

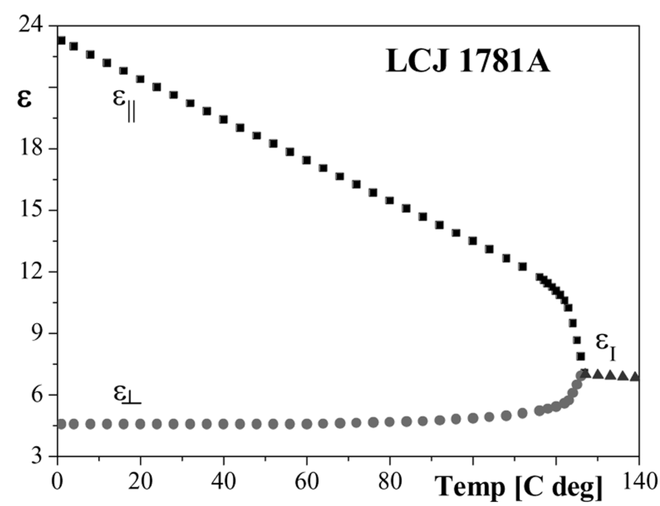

Figure 13. Temperature dependence of $\varepsilon_{||}(T)$, $\varepsilon_{\perp}(T)$ and $\varepsilon_I(T)$ for LCJ1791A at f = 1.0 kHz.

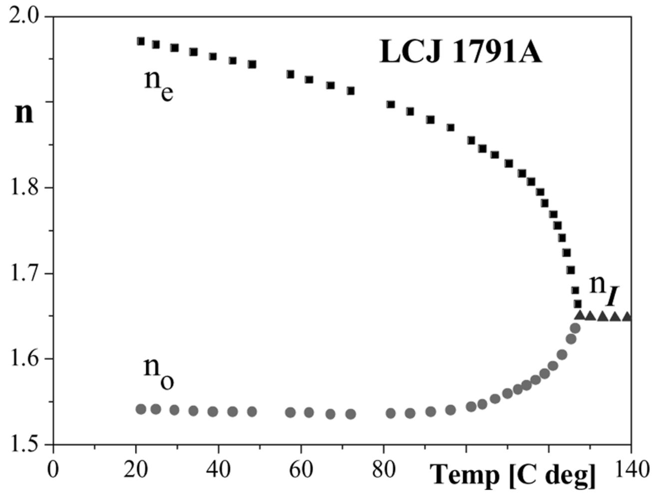

Figure 14. Temperature dependence of $n_e(T)$, $n_o(T)$, and $n_I(T)$ for LCJ1791A at $\lambda = 0.589\,\mu m$.

refractometers (ATAGO 2T.Hi and ATAGO 4T) and different kinds of interference wedges [9,10]. Values of $n_I(T)$, $n_o(T)$, and n_e (T) are presented graphically in Figure 14.

Figure 15 shows the dispersion of optical anisotropy $\Delta n(\lambda)$ for LCJ1791A in the visible range of λ. The some points of presented in Figure 15 dispersion $\Delta n(\lambda)$ were measured directly (using both Abbe refractometers and wedges cells) for standard λ (0.481 μm, 0.546 μm, 0.589 μm, 0.633 μm) while the other ones were calculated from (3) on experimental plots $T(\lambda)$ obtained in birefringent systems for different thicknesses d with $U = 0\,V$ (as it is seen in Fig. 16).

Splay ($K_{11} = 23pN$) elastic constant of LCJ1791A was estimated from observation Freedericksz transition under voltage U in HG cell monitored by dielectric measurements (see Fig. 17).

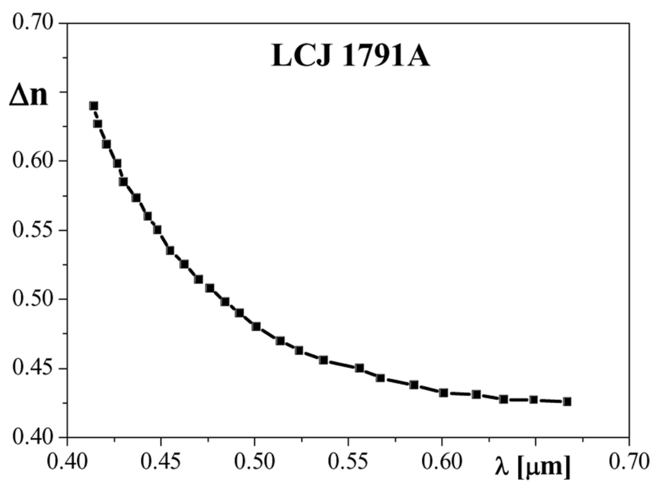

Figure 15. Dispersion of optical anisotropy $\Delta n(\lambda)$ for LCJ1791A.

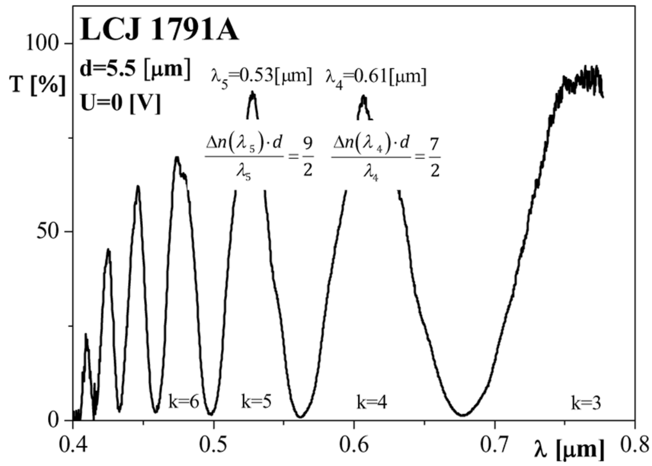

Figure 16. Transmission T(λ) of LCJ1791A in birefringent system (d = 5.5 μm, U = 0 V).

Viscosity γ was estimated from measuring switching time t_{ON} in LCJ1791A layer with $\Delta\varepsilon = \varepsilon_{\parallel} - \varepsilon_{\perp} = 15.0$, d = 8 μm in HG cell under U = 5 V [11]. Knowing that $t_{ON} = 2.5\ \tau_{ON}$ and taking into consideration (9) the value $\gamma = 150$cP was obtained.

Described above investigations show that of LCJ1791A, at room temperature, is characterized by: $n_o = 1.54$, $\Delta n = 0.43$ – for $\lambda = 0.633$ μm, $\varepsilon_{\perp} = 4.5$, $\Delta\varepsilon = 15.0$ – for f = 1 kHz, $\gamma = 150$cP and $K_{11} = 23$pN. Our LCJ1791A mixture satisfy all requirements for NLC formulated in chapter II, so our LCJ1791A can be used for manufacturing of proposed in this paper ETLCF. The physical properties obtained in this paper are in good agreement with data taken from [12–17].

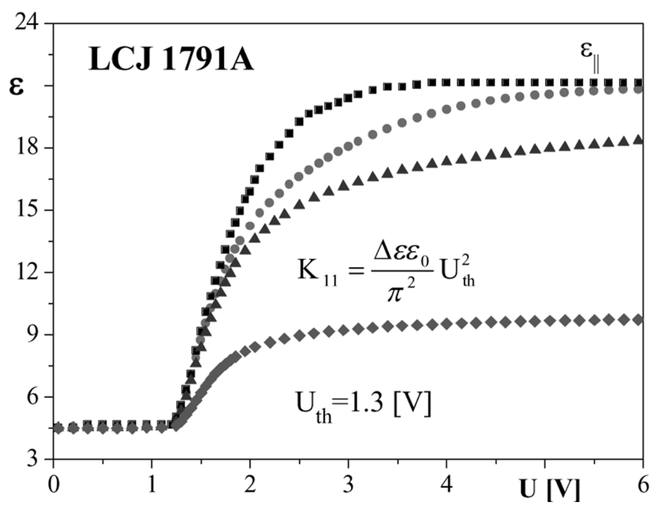

Figure 17. Freedericksz transition in planar cell under voltage U (d = 8 μm, $U_{th} = 1.3$ V, $\Delta\varepsilon = 15.0$, ε_0 – electric permittivity of the fee space), U_{th} – threshold voltage.

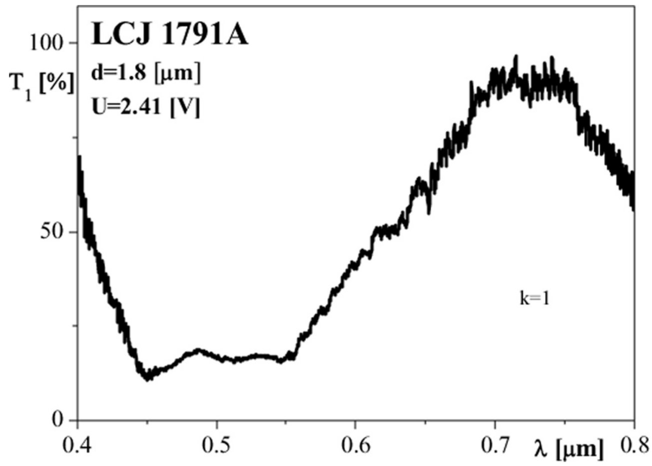

Figure 18. $T_1(\lambda)$ in 1.8HG for $U_1 = 2.41\,V$.

III. Experimental Results

To build ETLCF with mixture LCJ1791A, three HG cells with thicknesses $d = 1.8\,\mu m$, $d = 3.5\,\mu m$ and $d = 5.0\,\mu m$ (called: 1.8HG, 3.5HG and 5.0HG) were manufactured in our laboratory. The active area of ITO electrodes was $S = 25\,mm^2$. To obtain planar orientation, Nissan Polyimide Coating Homogenous Alignment SE-130 was used. The 1.8HG, 3.5HG and 5.0HG cells were filled by LCJ1791A in Iso phases and then the samples were slowly cooled from Iso to N phases, in the presence of low frequency (100 Hz) AC electric field (1 V/1 μm). The layout of ETLCF is shown in Figure 3. Three 1.8HG, 3.5HG and 5.0HG cells are sandwiched between four crossed polarizers. The effective birefringents of NLC layers in 1.8HG, 3.5HG and 5.0HG cells were guided by 100 Hz square waves with magnitudes U_1, U_2 and U_3 respectively. Three cells were supplied by three independent HP 33120A

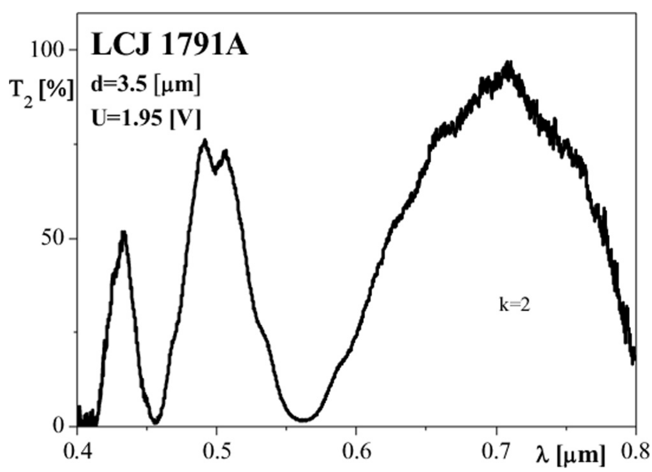

Figure 19. $T_2(\lambda)$ in 3.5HG for $U_2 = 1.95\,V$.

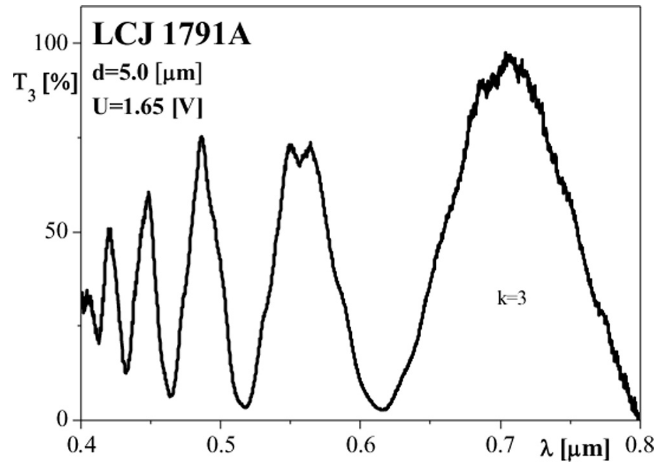

Figure 20. $T_3(\lambda)$ in 5.0HG for $U_3 = 1.65$ V.

Waveform Generators. The transmission spectra: $T_1(\lambda)$, $T_2(\lambda)$ any $T_3(\lambda)$ of 1.8HG, 3.5HG and 5.0HG cells placed between crossed polarizers and under different U_1, U_2 and U_3 voltages as well as the transmissions $T_F(\lambda)$ of all ETLCF were collected by using CCD Spectrometer BRC111A USB-VIS, driven by PC. During the transmission measuring processes, the temperature ($22.0 \pm 0.2°C$) of ETLCF was controlled by specially prepared hot stage.

Figures 18–20 show the transmission spectra $T_1(\lambda)$, $T_2(\lambda)$, and $T_3(\lambda)$ of 1.8HG, 3.5HG and 5.0HG cells (placed between crossed polarizers) under $U_1 = 2.41$ V, $U_2 = 1.95$ V, and $U_3 = 1.65$ V, respectively. When above listed voltages are applied to the proper cells, one observes the first interference maximum (with $k = 1$, see Fig. 18) in 1.8HG cell, the second maximum (with $k = 2$, see Fig. 19) in 3.5HG cell and the third one (with $k = 3$, see Fig. 20) in 5.0HG one at the same wavelengths $\lambda = 0.70\,\mu m$. As the results of it in the transmission $T_F(\lambda)$ of ETLCF under

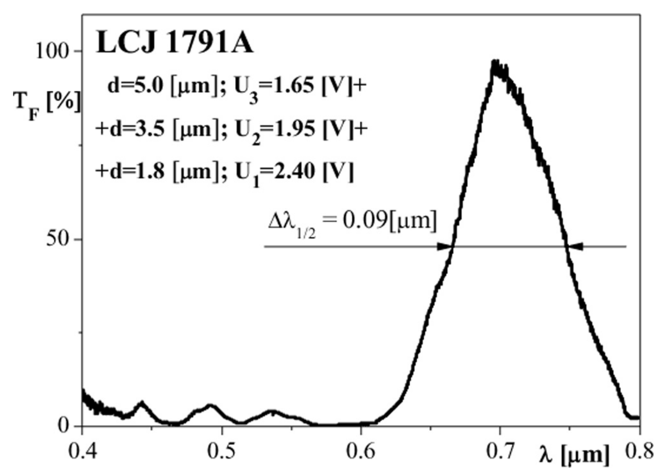

Figure 21. $T_F(\lambda)$ for $U_1 = 2.40$ V, $U_2 = 1.95$, $U_3 = 1.65$ V.

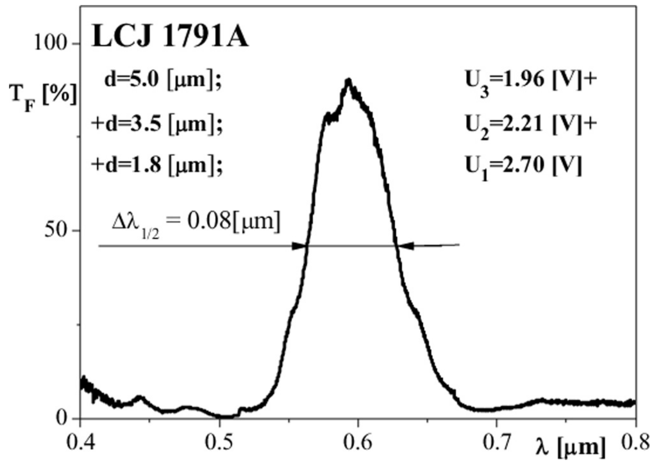

Figure 22. $T_F(\lambda)$ for $U_1 = 2.70$ V, $U_2 = 2.21$, $U_3 = 1.96$ V.

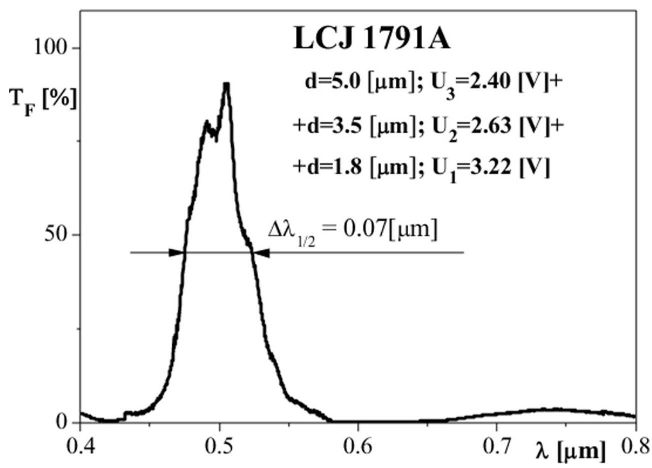

Figure 23. $T_F(\lambda)$ for $U_1 = 3.22$ V, $U_2 = 2.63$, $U_3 = 2.40$ V.

Table 1. Voltages U_1, U_2, and U_3 allowing transmission of ETLCF at chosen wavelengths

	$\lambda_1 = 0.70\,\mu m$	$\lambda_2 = 0.65\,\mu m$	$\lambda_3 = 0.60\,\mu m$	$\lambda_4 = 0.55\,\mu m$	$\lambda_5 = 0.50\,\mu m$
U_1 [V]	2.40	2.57	2.70	2.85	3.22
U_2 [V]	1.95	2.09	2.21	2.42	2.63
U_3 [V]	1.65	1.80	1.96	2.21	2.40

$U_1 = 2.41$ V, $U_2 = 1.95$ V, and $U_3 = 1.65$ V one observes only one transmission band at $\lambda = 0.70\,\mu$m in the all visible range, what is shown in Figure 21. When the other set of voltages (U_1, U_2, and U_3) are chosen, listed in Table 1, one can obtain the other λ band-pass (see Table 1 and Figs. 22 and 23.). Since the guided functions $\lambda = f(U_1)$, $\lambda = f(U_1)$, $\lambda = f(U_1)$ defined in Table 1 are near linear ones, our ETLCF can be a device whose spectral transmission can be uniform continuously controlled by applying voltages.

Our measurements show that, the maximum intensity of the light transmitted through our three HG cells of ETLCF reaches only 16% of incident light.

IV. Conclusions

In spite of the fact that ETLCF has got rather wide $\Delta\lambda_{1/2}$ in visible and near infrared spectral range, ETLCF can gain wide acceptance (eg. in astronomy and remote sensing pollution monitoring). A distinct advantage of ETLCF over conventional tunable filters is the possibility of construction such filter with extremely large clear aperture, low power consumption and low addressing voltage. There is the theoretical possibility to obtain ETLCF with much narrower bands (with $\Delta\lambda_{1/2} \approx 0.04\,\mu$m) by adding to the existed stack of three LC cells one more 7HG cell, but the intensity of the light transmitted through our ETLCF can reach only a few percent (about 6%) of incident light.

Acknowledgments

This paper has been done in 2009 year under financial support the Polish Ministry of Sciences and Higher Education, Key Project POIG.01.03.01-14-016/08 "New Photonic Materials and their Advanced Application".

INNOVATIVE ECONOMY
NATIONAL COHESION STRATEGY

WAT

EUROPEAN UNION

References

[1] Crarke, D. & Grainger, J. F. (1971). *Polarized Light and Optical Measurements*, Pergamon Press: Oxford, UK.

[2] Born, M. & Wolf, E. (2003). *Principles of Optics, Seventh Edition – Electromagnetic Theory of Propagation, Interference and Diffraction of Light*, Cambridge University Press: London, UK.

[3] Pluta, M. (1993). *Advanced Light Microscopy, Volume 3 – Measuring Techniques*, Elsevier: Amsterdam, Nederland.

[4] Pluta, M. (1989). *Appl. Optics*, *28*, 1453.

[5] Kędzierski, J., Kojdecki, M. A., Raszewski, Z., Rutkowska, J., Piecek, W., Perkowski, P., Zieliński, J., & Miszczyk, E. (2008). *Opto-Electronic Review*, *16*, 390.

[6] Kędzierski, J., Kojdecki, M. A., Raszewski, Z., Zieliński, J., & Lipińska, L. (2005). *Proc. of SPIE*, *6023*, 602305-1.

[7] Liu, Y. J., Sun, X. W., Luo, D., & Raszewski, Z. (2008). *Applied Physics Letters*, *92*, 101114-1.
[8] Raszewski, Z., Kędzierski, J., Rutkowska, J., Zieliński, J., Żmija, J., Dąbrowski, R., & Opara, T. (1993). *Liquid Crystals*, *14*, 1959.
[9] Kędzierski, J., Raszewski, Z., Rutkowska, J., Piecek, W., Perkowski, P., Żmija, J., Dąbrowski, R., & Baran, J. W. (1996). *Mol. Cryst. Liq. Cryst.*, *282*, 205.
[10] Raszewski, Z., Kędzierski, J., Perkowski, P., Piecek, W., Rutkowska, J., Kłosowicz, S., & Zieliński, J. (2002). *Ferroelecrics*, *276*, 289.
[11] Morawiak, P., Piecek, W., Żurowska, M., Perkowski, P., Raszewski, Z., Dąbrowski, R., Czupryński, K., & Sun, X. W. (2008). *Opto-Electronic Review*, *17*, 40.
[12] Dabrowski, R., Dziaduszek, J., Ziółek, A., Szczuciński, Ł., Stolarz, Z., Sasnouski, G., Bezborodov, V., Lapanik, W., Gauza, S., & Wu, S. T. (2007). *Opto-Electronics Review*, *15*, 47.
[13] Gauza, S., Wen, C. H., Wu, B., Wu, S. T., Spadło, A., & Dąbrowski, R. (2006). *Liquid Crystals*, *33*, 705.
[14] Dąbrowski, R. (2004). *Mol. Cryst. Liq. Cryst.*, *421*, 1.
[15] Gauza, S., Wen, C. H., Wu, S. T., Janarthanan, N., Hsu, C. S. (2007). *Jpn. J. Appl. Phys.*, *479*, 169.
[16] Gauza, S., Wen, C. H., Wu, S. T., Zhao, Y., Ziółek, A., & Dąbrowski, R. (2006). *Mol. Cryst. Liq. Cryst.*, *453*, 215.
[17] Gauza, S., Zhao, Y., Cor, T. L., Wu, S. T., Ziółek, A., Dąbrowski, R., Catanescu, O., Chien, L. C., & Hsu, C. S. (2007). *Mol. Cryst. Liq. Cryst.*, *479*, 169.